The Effect of Sb Doping Concentration on Optical Properties of ZnO:Sb Thin Films by Sol-Gel Spin Coating Method

Motlan[1], Karya Sinulingga[2] and Nurdin Siregar[3]

Motlanm@unimed.ac.id[1], karyasinulinggakarya@unimed.ac.id[2], siregarnurdin@unimed.ac.id

Department of Physics, Faculty of Mathematics and Natural Sciences,
Universitas Negeri Medan, Indonesia[1,2,3]

Abstract. ZnO:Sb thin films with varying antimony (Sb) doping have been successfully synthesized using the so;-gel spin coating method. The results of XRD analysis of ZnO:Sb thin films with varying antimony (Sb) doping show a hexagonal wurtzite crystal structure with crystallite sizes decreasing from 16.27 to 15.14 nm along with increasing antimony doping concentration. The results of UV-Vis analysis show that increasing antimony (Sb) doping concentration is accompanied by decreasing transmittance values and increasing absorbance values of ZnO:Sb thin films. The energy band gap value of ZnO:Mg thin films ranges from 3.38 to 3.41 eV.

Keywords: sol-gel, spin coating, antimony (Sb), ZnO:Sb thin film.

1. Introduction.

To improve the physical, optical, and electrical properties of ZnO, variations in film thickness, heat treatment, and doping with metallic elements can be used. Some elements used as dopants include magnesium (Mg).[1], aluminum (Al)[2], antimony (Sb)[3], and others. ZnO thin films are also very promising because it has an energy bandwidth of 3.37 eV [4]and a binding energy of 60 meV and have good optical, electrical and piezoelectric properties.[5]. To improve the physical, optical, and electrical properties of ZnO, it can be engineered by varying the film thickness, heat treatment, and by doping with metal elements. This ZnO thin film can be synthesized with several very sophisticated equipment, such as molecular beam epitaxy (MBE), metal organic chemical deposition (MOCVD), RF sputtering, spray pyrolysis, and pulse laser deposition. However, the above methods have several disadvantages, such as expensive equipment costs and a higher security system, considering the use of organic metals. Recently, ZnO thin films were synthesized by the sol-gel spin coating method.[6]and electroplating [7]. The preparation of ZnO samples doped with metal elements using sol-gel spin coating has shown significant progress. The efficiency of DSSCs made from ZnO-Mg only reached 3.53%.[8], ZnO-Cu reaches 2.03%[9], ZnO-Li[10], and others, which are generally still low and need to be improved. Recently, we have tried doping ZnO with antimony (Sb) and showed higher absorbance and transmittance values than ZnO with an Sb atomic concentration of around 3%. Therefore, researchers want to find parameters that produce maximum optical properties so that they can improve the efficiency of ZnO:Sb DSSCs better.

ICIESC 2025, September 16, Medan, Indonesia

DOI 10.4108/eai.16-9-2025.2361151

2. Method

ZnO:Sb thin films were synthesized using the sol-gel spin coating method. The research materials used were Zinc Acetate Dehydrate, Sb, Isopropanol, and Diethanolamine, each as a base material, solvent, and stabilizer. *Acetate dehydrate* {Zn(CH3COOH).2H2O} doped with antimony (Sb) is dissolved in isopropanol solvent, then stirred with a magnetic stirrer, and after 10 minutes, it is added into the solution little by little. *Diethanolamine (DEA).* The gel-like solution was then dripped onto an FTO glass substrate and rotated at a rotational speed of 5000 rpm. The sample was then heated to the required heating temperature. Pre-heating *at* 2500 °C for 5 hours and post-heating at 500°C for 5 hours with a heating holding time of 30 minutes. The ZnO:Sb thin film samples were then characterized by XRD and UV-Vis.

3. Results and Discussion

3.1. Crystal Structure of ZnO:Sb Thin Films with Variations of Antimony (Sb) Doping

ZnO:Sb thin film samples with varying Sb doping concentrations (2%, 2.5%, 3%, 3.5%, and 4%) which were characterized by XRD results, diffraction pattern shown in Figure 1. The results of the XRD pattern analysis for all samples have the same crystal planes, namely (100), (002), and (101), with the main peak oriented on the (101) plane. The c/a ratio for all samples has the same value as the ideal value for hexagonal cells c/a = 1.602 [10]. These results indicate that the crystals are hexagonal wurtzite and are in accordance with the ZnO standard data JCPDS card No. 36-1451. These results also show that variations in antimony doping concentration do not change the crystal structure.

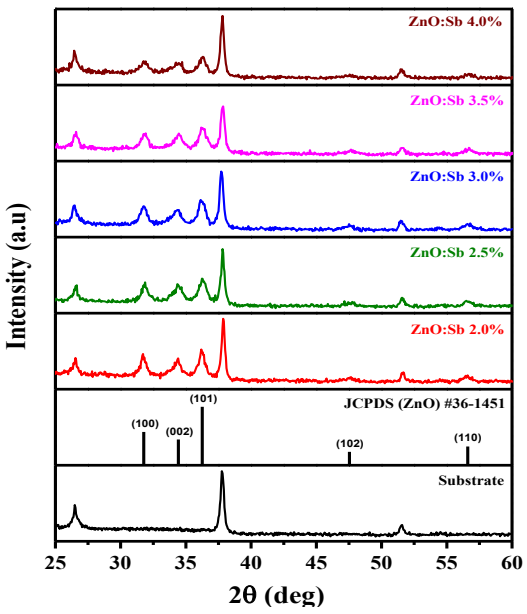

Fig. 1. X-ray diffraction spectra of ZnO:Sb

The crystallite size of ZnO:Sb thin films with varying antimony (Sb) doping concentrations, the results of which are shown in Table .1.

Table 1. Crystalline Size of ZnO:Sb Thin Films with Variation of Sb Doping

Samples	Crystal Size (nm)
ZnO:Sb 2.0%	16.27
ZnO:Sb 2.5%	15.81
ZnO:Sb 3.0%	15.70
ZnO:Sb 3.5%	16.27
ZnO:Sb 4.0%	15.14

Based on Table 1, it can be seen that the crystal size is getting smaller from 16.27 to 15.14 nm. along with increasing antimony doping concentration. This is in accordance with research results [11]. This result can be explained by the introduction of Sb into ZnO cells, which causes the incorporation of Sb into ZnO, thereby increasing the stress and causing the fracture of ZnO crystals, resulting in smaller crystallite sizes. Therefore, the small crystallite size can cause quantum dot regime and Blue Shift events due to Sb doping, and is mostly ascribed to the Burstein-Moss effect, which is the increase in the optical band gap energy value of ZnO:Sb [12].

3.2 Optical Properties of ZnO:Sb Thin Films

Transmittance and absorbance spectra for ZnO:Sb with varying antimony (Sb) doping concentrations, UV-Vis test resultsin the range of 300-700 nm shown in Figure 2.

(a) **(b)**

Fig. 2. (a) Absorbance Spectrum of Sb Doping Variation, and (b) Transmittance Spectrum Sb Doping Variations

Figure 2a shows an increase in absorbance in the ZnO:Sb thin film as the Sb doping concentration increases. The highest absorbance spectrum value is 0.89 au at an antimony (Sb) doping concentration of 3.5% and the lowest is 0.83 au at an antimony (Sb) doping concentration of 4.0%. In the transmittance spectrum (Figure 2b), it is seen that the ZnO:Sb thin film experiences a decrease in transmittance as the antimony (Sb) doping concentration increases. A higher transmittance spectrum is shown by the ZnO:Sb thin film with 2% Sb doping, this high transmittance can be attributed to the reduction of defects and increased regularity of the c

Crystal structure due to Sb doping, which allows more light to pass through the thin film. In contrast, there is a slight shift in the absorption edge and transmittance edge around 350 nm to 380 nm towards shorter wavelengths as the Sb doping concentration increases, indicating a change in the optical properties of the ZnO:Sb thin film. This indicates a change in the band gap energy in the ZnO thin film with Sb doping.

For materials with a direct band gap, the relationship between absorbance and photon frequency and based on the Tauc Plot method, and the energy band gap of ZnO:Sb thin films with variations in antimony (Sb) doping is obtained as shown in Figure 3.

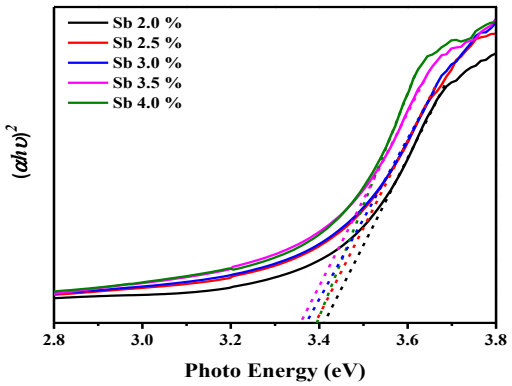

Fig. 3. Energy Band Gap of ZnO:Sb

Based on Table 2, the band gap values of ZnO thin films and variations in Sb doping show an interesting trend. The highest band gap value for ZnO:Sb with 2% antimony (Sb) doping is 3.41, which is a typical characteristic of ZnO:Sb with a hexagonal wurtzite structure according to SEM and HRD results. Increasing the antimony (Sb) doping concentration is accompanied by a decrease in the band gap value to 3.38 eV, and increases to 3.40 eV at 4% doping. This decrease can be caused by several factors, such as the appearance of crystal defects or the insertion of excess Sb atoms into the ZnO lattice, which causes distortion of the crystal structure. When the doping concentration is too high, the interaction between Sb atoms and the ZnO structure can cause a decrease in crystal order and an increase in the number of defects, such as Zn or oxygen vacancies. These defects can act as electron-trapping centers, reducing the effectiveness of increasing the band gap [13] [14]. The decrease in the band gap value is likely due to the stronger carrier scattering effect at high doping concentrations, which hinders electron mobility and affects energy transitions [15].

Table 2. Energy band gap of ZnO:Sb

Sample	Bandgap (eV)
ZnO:Sb (2.0%)	3.41
ZnO:Sb (2.5%)	3.40
ZnO:Sb (3.0%)	3.39
ZnO:Sb (3.5%)	3.38
ZnO:Sb (4.0%)	3.40

The successful synthesis of ZnO:Sb thin films via the sol-gel spin coating method demonstrates the viability of this cost-effective approach for producing doped semiconductor materials with tunable optical properties. The hexagonal wurtzite structure observed across all doping concentrations confirms the structural stability of ZnO despite antimony incorporation, which aligns with findings that Sb doping maintains the wurtzite crystalline phase without inducing structural transformation [16]. The preservation of the crystalline structure while varying dopant concentration is crucial for maintaining the fundamental electronic properties that make ZnO attractive for optoelectronic applications.

The observed decrease in crystallite size from 16.27 nm to 15.14 nm with increasing Sb doping concentration represents a significant structural modification that directly impacts the material's optical behavior. This reduction can be attributed to the ionic radius mismatch between Sb^{3+} (0.76 Å) and Zn^{2+} (0.74 Å), which introduces lattice strain and disrupts crystal growth. The crystallite size reduction mechanism in sol-gel derived ZnO is influenced by grain boundary density and porosity, where dopant atoms preferentially segregate at grain boundaries and inhibit further crystal growth [17]. Recent investigations on doped ZnO systems reveal that structural features such as reduced crystallite size and increased grain boundaries directly impact charge transport and dielectric response, which are critical for device performance [18]. The accumulation of Sb atoms at grain boundaries can effectively inhibit grain growth during the annealing process, leading to a refinement of the crystallite structure.

The quantum confinement effects arising from reduced crystallite sizes play a crucial role in the observed optical properties. When crystallite dimensions approach the exciton Bohr radius of ZnO (approximately 2.34 nm), quantum confinement becomes significant, leading to modifications in the electronic band structure. Although the crystallite sizes in this study remain above this threshold, the systematic reduction still influences the density of states and carrier dynamics within the material. The blue shift observed in the absorption edge with increasing Sb doping can be partially attributed to these size-dependent effects combined with the Burstein-Moss effect.

The Burstein-Moss effect becomes prominent when Sb doping introduces additional charge carriers into the conduction band, filling lower energy states and forcing optical transitions to occur at higher energies [19]. This effect is particularly relevant at lower doping concentrations (2.0-2.5%), where the band gap reaches its maximum value of 3.41 eV. Studies on doped ZnO have demonstrated that increased carrier concentration shifts the Fermi level

upward in the conduction band, resulting in band filling which manifests as an increase in the energy gap [20]. However, the subsequent decrease in band gap energy at higher doping concentrations (3.0-3.5%) reveals competing mechanisms at play. The introduction of excessive Sb atoms creates point defects, including oxygen vacancies and zinc interstitials, which form localized states within the band gap. These defect states act as intermediate energy levels that facilitate sub-band gap transitions, effectively narrowing the observed optical band gap.

The non-monotonic behavior of the band gap, where it decreases from 3.41 eV to 3.38 eV and then increases slightly to 3.40 eV at 4.0% doping, suggests a complex interplay between quantum confinement, the Burstein-Moss effect, and defect-related phenomena. At optimal doping levels (2.0-2.5%), the enhancement of carrier concentration dominates, leading to band gap widening. However, as the doping concentration increases beyond 3.0%, the accumulation of structural defects and the formation of Sb-related complexes begin to compensate for the Burstein-Moss effect. Research indicates that the conductivity and band gap behavior in Sb-doped ZnO are closely affected by dopant concentration, with variations in resistivity and lattice parameters relating directly to carrier transport mechanisms [21]. This defect compensation mechanism has been observed in heavily doped ZnO systems, where excessive dopant concentration leads to clustering and secondary phase formation.

The transmittance and absorbance characteristics of ZnO:Sb thin films reveal important insights for photovoltaic applications. The highest transmittance at 2.0% Sb doping indicates optimal crystal quality with minimal defect scattering, making this composition particularly suitable for transparent conductive oxide applications. Enhanced optical performance in antimony-doped ZnO has been demonstrated for UV photodetector applications, where maintaining the hexagonal wurtzite structure is crucial for device efficiency [22]. The increased absorbance at 3.5% doping (0.89 au) suggests enhanced light-matter interaction, which could benefit photon harvesting in solar cell applications. However, the trade-off between transparency and absorption must be carefully balanced based on the specific application requirements.

The slight blue shift in both absorption and transmission edges toward shorter wavelengths with increasing Sb doping concentration indicates modifications in the electronic structure that extend beyond simple band gap changes. This spectral shift can be attributed to changes in the local electronic environment caused by Sb incorporation, which alters the crystal field and spin-orbit coupling parameters. Spectroscopic investigations have revealed that antimony incorporation produces strong optical transitions related to free-electron to acceptor level transitions, which exhibit temperature-dependent behavior [23]. The optical properties modification demonstrates the potential for band gap engineering through controlled Sb doping.

From a technological perspective, the results suggest that ZnO:Sb thin films with 2.0-2.5% doping concentration offer the best compromise between optical transparency and band gap optimization for photovoltaic applications. The relatively high band gap values (3.38-3.41 eV) make these materials suitable for UV photodetectors and transparent electronics. For dye-sensitized solar cells (DSSCs), the moderate absorbance and high transmittance at lower doping concentrations could facilitate efficient light penetration to the dye layer while maintaining good electron transport properties.

The sol-gel spin coating method proves advantageous for producing ZnO:Sb thin films with controllable properties at lower costs compared to vacuum-based techniques. The ability

to fine-tune optical properties through simple dopant concentration variation offers a practical pathway for optimizing device performance in various optoelectronic applications.

4. Conclusion

The synthesis of ZnO:Sb thin films with varying antimony doping concentrations (2.0, 2.5, 3.0, 3.5, and 4%) has been successfully carried out using the sol-gel spin coating method. The crystal structure of ZnO:Sb thin films with varying Sb doping is wurtzite hexagonal and increasing antimony (Sb) concentration is accompanied by a decrease in crystal size from 37.5 to 15.8 nm. The highest absorbance spectrum value is 0.89 au at an antimony (Sb) doping concentration of 3.5% and the lowest is 0.83 au at an antimony (Sb) doping concentration of 4.0%. The transmittance spectrum of ZnO:Sb thin films decreased with increasing antimony (Sb) doping concentration. The transmittance spectrum was higher at 2% Sb doping. The largest band gap value is at a Sb doping concentration of 2% and the smallest is at a Sb doping concentration of 3.5%. The energy band gap ranges from 3.38 to 3.41 eV.

Acknowledgments.

The researcher would like to thank the leadership of Unimed for the encouragement and support of the PNBP funds from Medan State University for the 2024 Fiscal Year, with contract number:0194/UN33.8/PPKM/PPT/2025, so that this research can be completed.

References

[1]. N. Siregar, Motlan, and J. Panggabean, "The effect of magnesium (Mg) on structural and optical properties of ZnO:Mg thin film by sol-gel spin coating method," in Journal of Physics: Conference Series, 2020. doi: 10.1088/1742-6596/1428/1/012026.

[2] N.Siregar, Motlan, and JH Pangabean, "Effect of Post-Heating Temperature on Efficiency of Dye-Sensitized Solar Cell with ZnO:Al Thin Films Prepared by Sol-Gel Spin Coating," Journal of Physical Science, 2021, doi: 10.21315/jps2021.32.2.5.

[3] N.Siregar, M. Sirait, and Motlan, "Synthesis and optical properties of Sb-doped ZnO thin film by sol-gel spin coating method," in Journal of Physics: Conference Series, 2022. doi: 10.1088/1742-6596/2193/1/012063.

[4] W.Amananti, R. Ardiyanto, H. Sutanto, I. Nurhasanah, and I. Tivani, "Analysis of the optical properties of ZnO thin films deposited on a glass substrate by the So-gel method," Journal of Natural Sciences and Mathematics Research, 2022, doi: 10.21580/jnsmr.2022.8.1.9623.

[5] R. Sha, A. Basak, PC Maity, and S. Badhulika, "ZnO nano-structured based devices for chemical and optical sensing applications," Sensors and Actuators Reports, 2022, doi: 10.1016/j.snr.2022.100098.

[6]. W. Cheng et al., "Global monthly gridded atmospheric carbon dioxide concentrations under the historical and future scenarios," Scientific Data, 2022, doi: 10.1038/s41597-022-01196-7.

[7] TMN Vo, CN Wang, FC Yang, and VTT Nguyen, “Renewal Energy Efficiency Assessment,” in*Eurasia Proceedings of Science, Technology, Engineering and Mathematics*, 2023. doi: 10.55549/epstem.1374936.

[8] S.Shukrullah, MY Naz, K. Ali, and SK Sharma, “Carbon Nanotubes: Synthesis and Application in Solar Cells,” in Solar Cells: From Materials to Device Technology, 2020. doi: 10.1007/978-3-030-36354-3_7.

[9] R. Parasuraman, “High Photo Switching Response of n-ZnO/i-MoS2/p-Si Heterojunction Solar Cel,” Journal of Computational Electronics, 2021.

[10] K.Mykhailo, Z. Roman, K. Gennadiy, M. Kseniia, T. Roman, and P. Dmytro, “Influence of Functional Layers Thickness on CdTe Based Flexible Solar Cells Efficiency,” in Proceedings of the International Conference on Advanced Optoelectronics and Lasers, CAOL, 2019. doi: 10.1109/CAOL46282.2019.9019415.

[11]. Sridevi, D. and Rajendran, KV. 2009. Synthesis and Optical Characteristics of ZnO Nanocrystals, Bull Mater Sci., 32. Indian Academy of Sciences.

[12]. Rouchdi, M., E. Salmani., B. Fares., N. Hassanain., A. Mzerd. (2017). Synthesis and characteristics of Mg doped ZnO thin films: Experimental and ab-initio study. Results in Physics. Elsevier.

[13] Sathya, M., Claude, A., Gavindasamy, P. and Sudha, K. 2012. Growth of Pure and Doped ZnO Thin Films for Solar Cell Applications. Pelagia Research Library. Advanced in Applied Science Research Vol 3.

[14]. Lee, J.C. et al. (2000). RF sputter deposition of the high-quality intrinsic and n-type ZnO window layers for Cu(In,Ga)Se2-based solar cell applications. Sol. Energy Matters. Sol. Cells, 64(2), 185–195. https://doi.org/10.1016/S0927-0248(00)00069-6

[16]. Justin, RC, Kandasamy Prabakar., Karthick SN, Hemalatha KV, Min -Kyu Son., and Hee-Je Kim. (2013). Banyan Root Structured Mg Doped ZnO Photoanode Dye Sensitized Solar Cells. J Phys. Chem. C, Just Accepted Manuscript • DOI: 10.1021/jp308847g • Publication Date (Web)

[16] Bhat, M.A., R.A. Rather, and A.H. Shalla, "Enhanced optical and electrical properties of antimony doped ZnO nanostructures based MSM UV photodetector fabricated on a flexible substrate," Sensors and Actuators A: Physical, vol. 296, pp. 24-34, 2019. doi: 10.1016/j.sna.2019.06.049.

[17] Kumar, A., R. Singh, and B.C. Yadav, "Sol–gel synthesized zinc oxide nanorods and their structural and optical investigation for optoelectronic application," Scientific Reports, vol. 14, 5042, 2024. doi: 10.1038/s41598-024-55135-5.

[18] Sharma, P., S. Kumar, and M. Singh, "Sol–gel derived ZnO nanoparticles doped with transition and alkaline-earth metals: a comprehensive review on dielectric and electrical properties," Journal of Sol-Gel Science and Technology, vol. 113, pp. 1-28, 2025. doi: 10.1007/s10971-024-06545-0.

[19] Zhou, L., Y. Wang, and H. Zhang, "Engineering of Optical and Electrical Properties of Electrodeposited Highly Doped Al:ZnO and In:ZnO for Cost-Effective Photovoltaic Device Technology," Materials, vol. 15, no. 22, 8129, 2022. doi: 10.3390/ma15228129.

[20] Kim, S., J. Park, and W. Lee, "Tuning the Optical and Electrical Properties of ALD-Grown ZnO Films by Germanium Doping," Materials, vol. 17, no. 11, 2677, 2024. doi: 10.3390/ma17112677.

[21] Mahdi, M.A., J.J. Hassan, and S.S. Ahmed, "Effect of Sb doping on the electrical and dielectric properties of ZnO nanocrystals," Ceramics International, vol. 45, no. 3, pp. 3820-3825, 2019. doi: 10.1016/j.ceramint.2018.11.048.

[22] Singh, R., N. Kumar, and R.K. Shukla, "Enhanced optical and electrical properties of antimony doped ZnO nanostructures based MSM UV photodetector fabricated on a flexible substrate," Sensors and Actuators A: Physical, vol. 296, pp. 24-34, 2018. doi: 10.1016/j.sna.2019.06.049.

[23] Meral, K., and L. Arda, "Influence of Antimony doping on the electronic, optical and luminescent properties of ZnO microrods," Materials Science in Semiconductor Processing, vol. 88, pp. 86-93, 2018. doi: 10.1016/j.mssp.2018.08.003.